Thermoelectric generators for long duration lunar missions

*Pol Serra * and Ricard González-Cinca***
**Department of Physics, Universitat Politècnica de Catalunya-BarcelonaTech*
c/ E. Terradas, 5, 08860 Castelldefels, Barcelona (Spain), pooolse4@gmail.com
*** Department of Physics, Universitat Politècnica de Catalunya-BarcelonaTech*
c/ E. Terradas, 5, 08860 Castelldefels, Barcelona (Spain), ricard.gonzalez@upc.edu

Abstract

The number of lunar missions involving the deployment of probes, rovers and other equipment is expected to raise significantly. Some of these missions will face the challenge to survive the night on the Moon, with very low temperatures on the surface. Solar thermal energy can be stored during the day and transformed into electricity at night. We present a study of the performance of thermoelectric modules. Some of the modules are used in simulations of a thermal energy storage system, which includes the test of different materials as a thermal mass. The power generated in all the cases is obtained.

1. Introduction

The interest to carry out lunar missions in the coming years is increasing. One of the main concerns for medium and long term missions is the availability of power and heat during the night. Technologies such as batteries, hydrogen cells and thermochemical processes could be considered as an option for energy storing. However, they might be neither a sustainable nor a scalable solution given the high costs of transporting equipment to the Moon. In-Situ Resource Utilisation (ISRU) is currently a promising alternative to be considered in the future of the lunar exploration.

Several studies have been recently carried out to develop technologies capable of supplying the required power in a lunar outpost during lunar nights relying on ISRU [1-3]. Heat collected from the solar illumination is stored during the day in thermal masses and used during the night to generate electricity or to warm equipment. Thermoelectric materials are a choice to consider for the heat-to-electricity conversion [4, 5]. Here we analyse the use of thermoelectric modules to convert the heat from the thermal mass into electricity, by exploring several combinations of thermoelectric materials working at different temperatures, including some which are potentially feasible to be crafted using ISRU.

In Section 2, the basis of the thermoelectric materials is described and set of thermoelectric couples and conductor materials are selected according to some defined criteria. The performance of the selected couples is analysed in Section 3. The open circuit voltage is determined both theoretically and by means of numerical simulations using COMSOL Multiphysics. Furthermore, the maximum efficiency and maximum generated power are obtained for a wide span of temperatures and a comparison between the couples is performed. Section 4 contains the modelling and simulation of the heat storage system in order to obtain the generated power. Three thermoelectric couples and three conductor materials are tested for the thermal mass. Conclusions are presented in Section 5.

2. Thermoelectric generators

Thermoelectric materials are able to generate a potential differential when they are exposed to a gradient of temperature. This capacity is determined by the Seebeck coefficient (S), which is positive for the p-type materials and negative for the n-type ones. By connecting p-type and n-type materials alternately in a series connection, significant levels of voltage can be obtained. Electric conductivity (σ) and thermal conductivity (κ) play an important role in thermoelectric materials. The figure of merit (ZT) is used to compare these material properties in terms of efficiency, which corresponds to the ratio between the electrical energy generated and the amount of heat absorbed by the hot side

of the generator. The higher ZT is the better the material will perform at a given range of temperatures. The figure of merit is defined according to the following expression:

$$ZT(\mathrm{T}) = S(T)^2 \frac{\sigma(T)}{\kappa(T)} \mathrm{T}, \quad \textbf{(1)}$$

with T being the temperature. The maximum efficiency is commonly used to rate and compare different generators and depends on the hot side and cold side temperatures (T_{hot} and T_{cold}, respectively), and on the average of the figure of merit for the temperature range (ZT_{ave}):

$$\eta_{max} = \frac{T_{hot} - T_{cold}}{T_{hot}} \cdot \frac{\sqrt{1+ZT_{ave}} - 1}{\sqrt{1+ZT_{ave}} + \frac{T_{cold}}{T_{hot}}} \quad \textbf{(2)}$$

The maximum efficiency is only achieved when the internal electrical resistance of the generator (R_G) and the electrical resistance of the load connected to it (R_L) are related as [6]:

$$\frac{R_L}{R_G} = \sqrt{1 + ZT_{ave}} \quad \textbf{(3)}$$

Fig. 1 shows the maximum efficiency and the Carnot efficiency as a function of the temperature difference for different ZT.

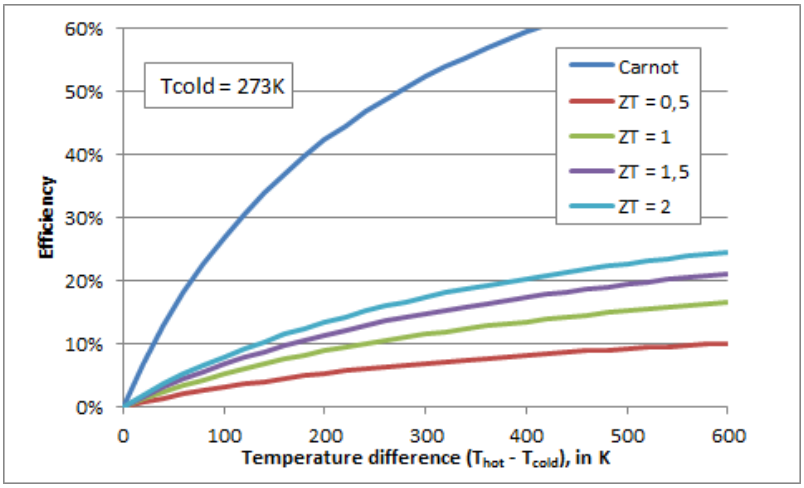

Figure 1**:** Efficiency for different values of ZT as a function of the difference of temperature (T_{cold} = 273 K).

The amount of power that a generator is able to produce is a key parameter to consider in the generator design, especially for sizing. The maximum transmitted power is reached when both R_L and R_G are the same and it is determined by:

$$P_{max} = \frac{N^2 S^2 (T_{hot} - T_{low})^2}{4R_G}, \quad \textbf{(4)}$$

N being the number of thermoelectric legs, which is also the number of electrical contacts.

2.1 Selected materials

Thermoelectric materials are under an increasing development and it is expected that new materials with higher performances will be developed in the future. In order to select the materials for this study, five categories have been considered: very high temperature, high temperature, medium-low temperature, ISRU feasible, and alternative/low cost. For each category, the materials with the best ZT have been selected. All the selected materials are under research and perform better than the ones currently in use. The aim behind this selection is to simulate the performance of future

materials, as the real application of this technology on the Moon would take place in the future. The selected materials for each category, including both a n-type and a p-type for each category, are:

- Very high temperature (1): Materials that can endure temperatures up to 1150 K.
  - p-type: Nanostructured Silicon-Germanium [7] (1A-D)
  - n-type:
    - Nanostructured Silicon-Germanium [8] (1A)
    - Hot Pressed Nanostructured Silicon Germanium [9] (1B)
    - Praseodymium Telluride [10] (1C)
    - Barium Gallium Germanide clathrate [11] (1D)

- High temperature (2): Materials that can endure temperatures up to 900 K.
  - p-type: Bismuth Copper Oxyselenide [12] (2)
  - n-type: Lead Selenide – Lead Sulphide [13] (2)

- Medium – Low temperature (3): Materials that work usually with temperatures lower than 600 K.
  - p-type: Bismuth Antimony Selenide [14] (3)
  - n-type: Bismuth Selenium Telluride [15] (3)

- ISRU feasible (4): Materials made of elements that can be found on the surface of the Moon. The interest of these materials is that in the future they might be produced using the in-situ resources available.
  - p-type: 0.4% Gallium doped Silicon Magnesium [16] (4A-B)
  - n-type: 0 and 1.5% Bismuth doped Silicon Magnesium [17] (4A-B)

- Alternative/low cost (5): Complementary category to check the way low cost materials would perform. However, due to the current high cost of equipment transportation to the Moon, it might not be interesting to use low cost materials to the detriment of the performance.
  - p-type: Tellurium doped Celerium Iron Antimonide Skutterudite [18] (5)
  - n-type: Cobalt Antimonide Skutterudite [19] (5)

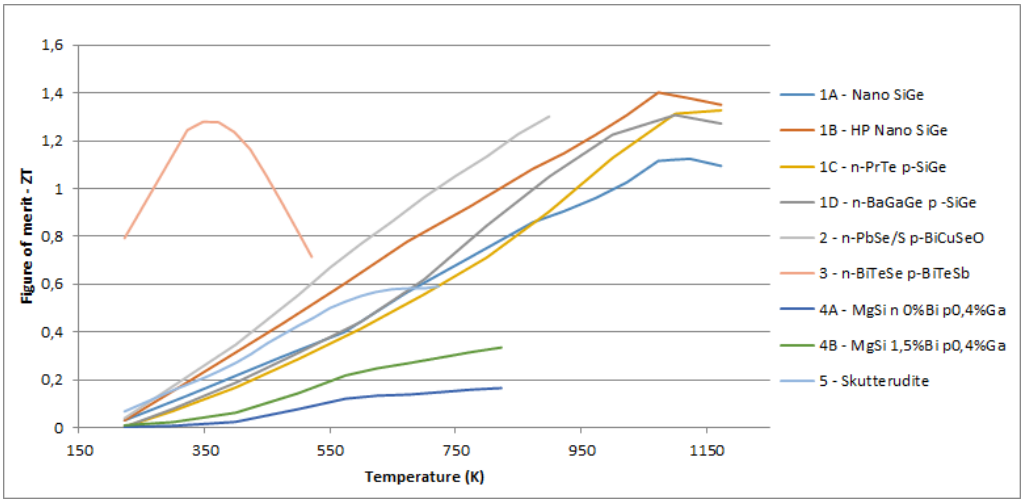

Figure 2: Figure of merit as a function of the temperature.

Numbers and letters in brackets correspond to the codes of the thermoelectric couples used in this study. For example, 1C refers to a thermoelectric couple made of a p-type Nanostructured Silicon-Germanium leg and an n-type Praseodymium Telluride leg. Fig. 2 shows the figure of merit as a function of the temperature obtained from the properties of the considered couples and Eq. 1. As expected, the couples of category (1) show the best performance at the highest temperatures. The potential ISRU materials have a significant worse performance whereas the low temperature couple has good properties when working around 350K.

A thermoelectric module is composed of several thermoelectric couples connected with each other through a conductor material with the n-legs and p-legs alternatively connected. The main constraint for connector materials is given by the

risk of getting too close to their melting temperature, where they soften, their properties are degraded, and eventually they melt. In order to avoid it, the connector materials used in this study are determined by the highest temperature endurable for each material. The materials used in each category are:

- Silver: $\sigma = 62.1 \times 10^6$ S/m, melting temperature = 961 K
  - Medium (3) – Low temperature: Maximum temperature = 500-550 K
  - IRSU feasible (4A and B): Maximum temperature = 823 K
  - Alternative/low cost (5): Maximum temperature = 723 K

- Copper: $\sigma = 58.5 \times 10^6$ S/m, melting temperature = 1083 K
  - High temperature (2): Maximum temperature = 900 K

- Nickel: $\sigma = 14.3 \times 10^6$ S/m, melting temperature = 1455 K
  - Very high temperature (1A to D): Maximum temperature above 1200 K

As regards to the design of the thermoelectric couple, the effects that might have in performance the length and width of the legs, the distance between them, or any other parameter, have not been considered in this work. The considered size of the legs and the connectors are taken from the most common ones in the market: 3mmx3mmx9mm and 9mmx3mmx0.5mm, respectively.

3. Thermoelectric module simulation

The aim of the simulations of the thermoelectric modules is to compare their performance in terms of maximum power, efficiency and specific power. In addition, theoretical computations of the open circuit voltage are compared with the COMSOL Multiphysics simulations, which take into account heat transfer and the Joule effect among other phenomena and losses.

3.1 Module simulation setup

Thermoelectric modules made of all the selected materials with the corresponding connectors were tested with 1, 72 and 256 thermocouples, labelled F, G (Fig. 3), and H, respectively. The cold side temperature is set to 273 K whereas the hot side temperature changes from 423 K to 1173 K in intervals of 50 K or 100 K, respecting the temperature limitations of the components.

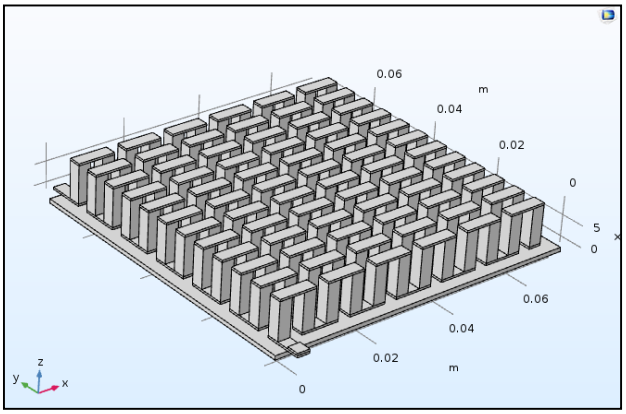

Figure 3: Size G module.

The internal electrical resistance of the modules has been computed theoretically and in order to obtain the maximum power from the generator the electrical resistance of the load has been set to the same value. Fig. 4 shows the internal electrical resistance for the modules of size G as a function of the hot side temperature. Data have been computed using the electrical conductivity of the materials and the shape and dimensions of the components. In general, all the couples have a similar variation with temperature and order of magnitude. However, the potential ISRU materials behave differently. The R_G of couple 4A is one order of magnitude higher than the rest. Moreover, R_G in couples 4A and 4B does not increase with temperature in all temperature ranges. In fact, the resistance always decreases with temperature in 4A.

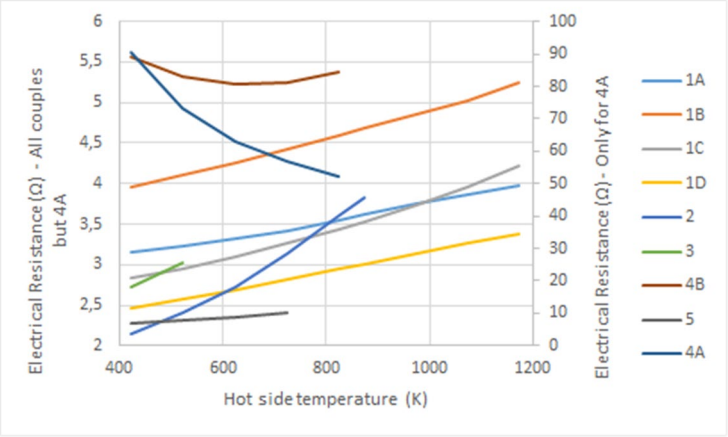

Figure 4: Internal electrical resistance of modules size G as a function of the hot side temperature (T_{cold} =273 K). Couple 4A follows right side scale.

3.2 Module simulation results

Fig. 5 shows the open circuit voltage obtained by means of the COMSOL simulations as a function of the hot side temperature. The voltage generated by couples 1 (A-D), 2 and 5 follow a similar positive slope as T_{hot} increases. Among this group, the material 1B is the one that provides the largest open circuit voltage at any temperature. Couple 3 obtains higher voltage outcomes within its working temperatures. However, due to its large Seebeck coefficient, the thermoelectric couple that produces the highest voltage is the potential ISRU couple 4A.

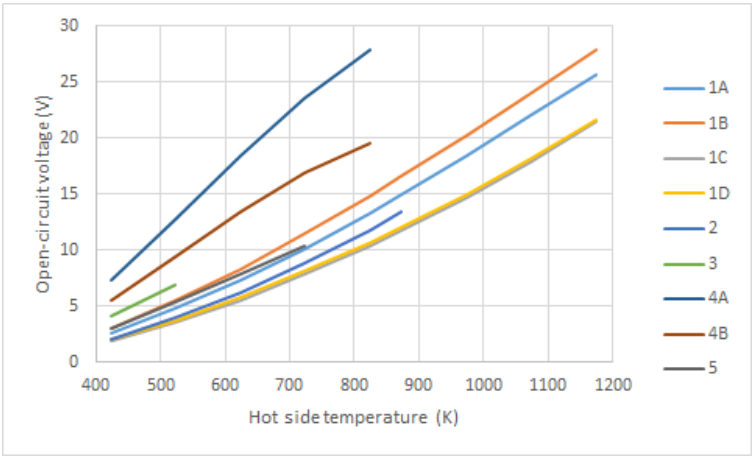

Figure 5: Open circuit voltage of each thermoelectric couple as a function of the hot side temperature from the COMSOL simulations.

Data shown in Fig. 5 have been compared with computations using the theoretical relations. Fig. 6 shows the relative error between the COMSOL simulations and the theoretical calculations. The relative error is always lower than 1.8%, and its highest values are reached by the very hot temperature couples at temperatures between 423 K and 723 K, which are not their usual working temperatures. When these data are neglected, the relative error is always below 0.6%. Furthermore, as the average error is 0.26% and in order to save computation time, all the further computations have relied upon the theoretical values. Regarding the modules of size F and H, they show a very similar behaviour in terms of voltage and relative error.

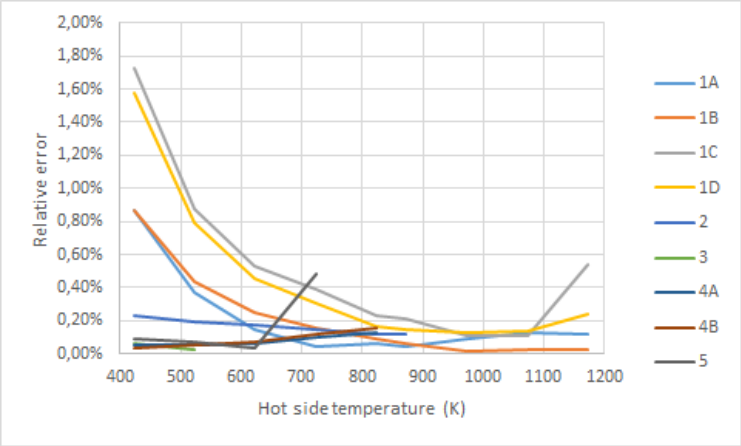

Figure 6: Relative error between COMSOL simulations and theoretical calculations as a function of the hot side temperature.

From the values of the open circuit voltage, the maximum power (Eq. 4, Fig. 7) and maximum efficiency (Eq. 2, Fig. 8) for a size G module as a function of the hot side temperature have been determined for all the thermoelectric couples. As the power output is proportional to the number of thermoelectric legs, the power output of a size H module would be 3.5 times the value of a size G module.

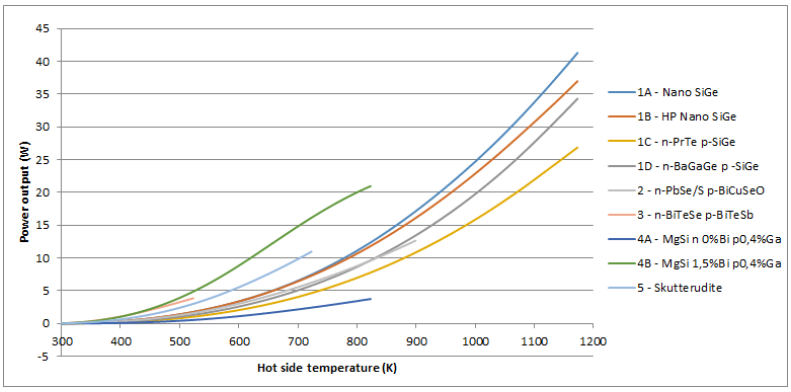

Figure 7: Maximum power output as a function of the hot side temperature.

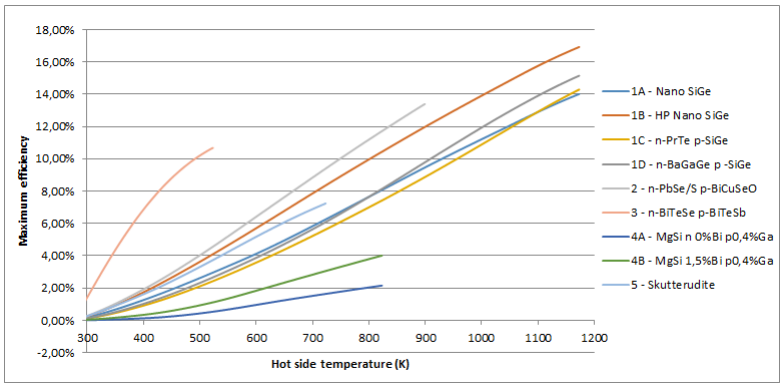

Figure 8: Maximum efficiency as a function of the hot side temperature.

Table 1 shows a comparison between the performance of the different thermocouples at three different temperatures according to the simulations. The temperature ranges evaluated are Very High temperature (above 900 K), High – Medium temperature (600 K to 850 K) and Medium-Low temperature (below 550 K). The evaluated characteristics are the maximum power, the maximum efficiency and the specific maximum power. The characteristics of each

thermoelectric couple have been evaluated comparing the one with the best properties with the others. The best thermocouple has a ++ score and progressively the others will score +, ~, - or - - in the worst case.

Table 1: Comparative of thermocouples. MP: Maximum power, Eff: efficiency, SpMP: Specific Maximum Power

Thot →	Above 900K			Between 850 and 600K			Below 550K		
Material	MP	Eff	SpMP	MP	Eff	SpMP	MP	Eff	SpMP
1A	++	+	++	+	~	+	-	-	+
1B	+	++	++	+	+	+	-	~	+
1C	~	+	~	-	~	-	-	-	-
1D	+	+	+	~	~	+	-	-	~
2				~	++	-	-	~	-
3							+	++	+
4A				- -	- -	-	- -	- -	-
4B				++	- -	++	++	- -	++
5							+	~	~

The four couples at Very High temperature have the same p-type material, which explains the similar performance they have. However, 1A and 1B couples surpass the other two couples. Thermocouple 1A provides the maximum power (41.3 W with a size G module at 1173 K), while 1B has the best maximum efficiency (up to 16.93% at 1173 K).

The additional thermocouples considered in the High-Medium temperature range are the ISRU ones and 2. Despite its low efficiency, ISRU couple 4B is able to provide the largest amount of power (17.6 W with a size G module at 823 K) while 4A has the poorest performance. Comparatively, the very hot temperature couples 1A and 1B are still a good option due to their balanced and good properties. Thermocouple 2 has the best efficiency (11.72% at 823 K), which is explained given it is working at its highest temperatures.

In the Medium-Low temperature range all the thermocouples tested are able to work. Since the High temperature thermocouples now work far from their optimal working temperatures, their properties are degraded to low power outputs and efficiencies. Thus, they should not be used at these temperatures. In the positive side, there is thermocouple 3, which has both a good power outcome and the best efficiency (3.6 W with a G size module and 10.7%, respectively, at 523 K). The potential ISRU couples behave similarly as they did at High-Medium temperatures. 4B shows the best power generation but a very poor efficiency (4.1 W with a G size module and 1.12%, respectively, at 523 K). 4A cuple behaves rather bad. Couple 5 would produce an amount of power similar to 3, but with worse efficiency and specific power.

The analysis of Table 1 provides information for the selection of the most adequate couple to use depending on the working temperature and the constraints of the system (power or efficiency). A clear conclusion from the analysis of the maximum efficiency and, especially, maximum power, is that the higher the working temperature the better the power outcome and the efficiency are. For instance, the power output from 1173 K to 823 K is reduced by a half, and it is ten times lower 523 K. Therefore, the thermal storage system should work at the highest possible temperature.

Despite the poor efficiency of the potential ISRU thermocouples, couple 4B is selected for the thermal mass simulations because of the relevancy of its possible production on the Moon. To be consistent with this selection, the thermal mass simulations are carried out at the High-Medium temperature range. Therefore, thermocouples 2 and 1A are selected as they have the best efficiency and best maximum power (excluding 4B), respectively.

4. Thermal storage system simulation

The performance of a small thermal energy storage system is simulated in the COMSOL environment, taking into account the transfer of heat and electric currents, and using results from the previous Sections. This means that the voltage generated is proportional not only to the temperature gradient but also to the actual heat crossing the generator. The objective of these simulations is to determine the power that the selected thermoelectric generators would be able to produce during the lunar night from the heat collected and stored in a thermal mass during the day. In addition to considering different thermoelectric couples, thermal masses made of different materials are tested to study their effect on the performance of the system.

The power output and efficiency have been theoretically computed using the theoretical electric resistances as a function of the temperature. The total power output will be the double of a single module for there would be two modules attached to the thermal mass.

4.1 System simulation setup

A thermal mass with a simple geometry and a small size is considered in order to simplify the simulations. The mass has a cylindrical shape with a radius of 0.25 m and a height of 0.4 m and it is surrounded by regolith to simulate the scenario in which the mass is buried. Regarding the thermoelectric modules and according to the size of the thermal mass, the size G modules are the ones that fit the best. After some preliminary simulations and analysis, it has been determined that two size G modules will be placed at the sides of the thermal mass, the furthest as possible from one another. Given the symmetry of the model and neglecting thermal losses caused by the proximity of the surface of the Moon, only one half of the thermal mass has been simulated, including one thermoelectric module. In order to fit the curved surface with the flat module, some extra material has been added as can be seen in Fig. 9. Notice that this is not the model used in the simulations but a preliminary one, as it is a third of the thermal mass instead of a half.

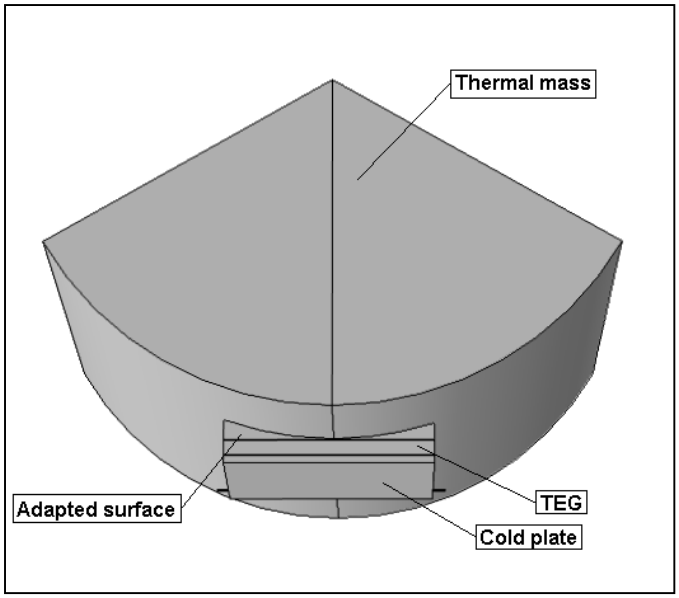

Figure 9: One third of the thermal mass with the coupled TEG and the adapted surface between them.

Neither the heat source system nor the heat rejection system have been modelled for the simulations. Instead, constant temperatures have been set at the cold plate of the generator and at the centre of the thermal mass. Even if during the lunar night the temperature at which the heat can be radiated on the surface is lower than 150 K [21], the heat rejection would not be able to keep such a cold temperature at the cold sink of the generator. Therefore, a temperature margin has been considered between the temperature on the surface and the temperature at the cold side of the generator, which is set to 250 K. The heat source at the centre of the thermal mass has been turned on during the lunar day (simulating the storage of heat) and turned off during the night (no power available, only discharge) and its temperature is set to 973 K.

In order to determine the initial temperature distribution at the regolith surrounding the thermal mass after some cycles (normal operation), two periods of thermal discharge and two of thermal charge have been simulated without the cold side heat sink.in these preliminary simulations, the initial temperature at the thermal mass and regolith was 973 K and 273 K, respectively. The discharge consisted in 354 hours without the heat source, and the charge consisted in the same time length with the heat source tuned on. The total duration of the preheating process was 1416 hours (2 lunar days or 59 Earth days). Fig. 10 shows the temperature distribution in the regolith before and after the pre-heating.

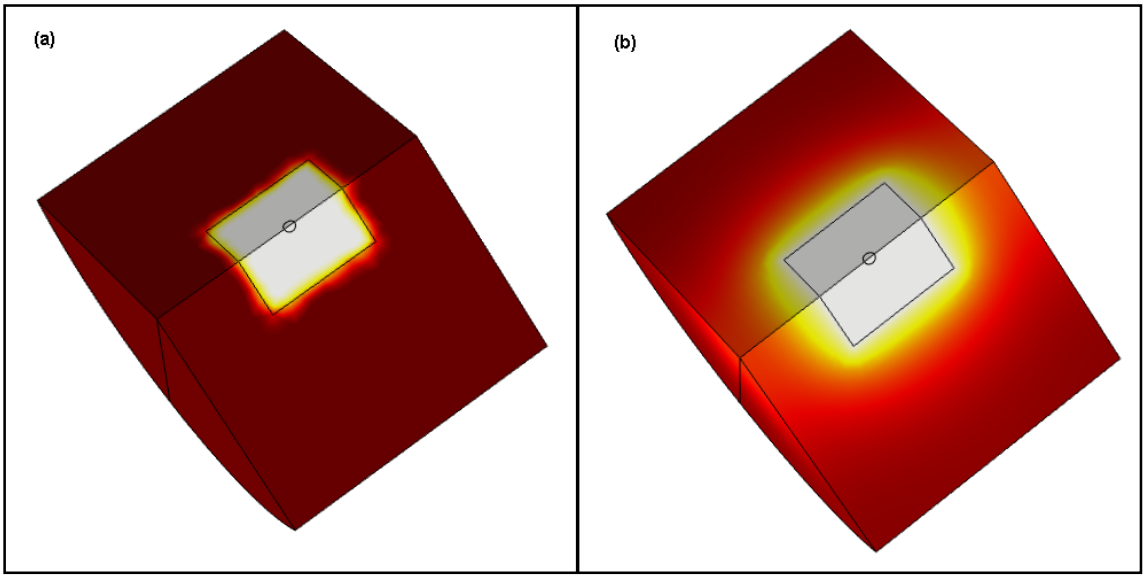

Figure 10: Temperature distribution at the beginning of the discharge, (a) without preheating and (b) with preheating.

Table 2 shows the properties of the materials tested for the thermal mass in the simulations.

Table 2: Properties of the materials used as a thermal mass in the simulations.

	Density (kg/m3)	Specific heat (J/kg·K)	Thermal conductivity (W/m·K)
Basalt rock	3000	800	2.10
Native regolith	1800	840	0.01
60% NaNO3 – 40 % KNO3	1733	1539	0.55

In this study, the basalt rock is frequently referred to as lunar rock and the NaNO3 – KNO3 just as salt. Notice that the native regolith is the same material used for the surrounding soil.

4.2 System simulation results

Fig. 11 shows the temperature of the hot side of the thermoelectric generator during the pre-heating phase for the three materials considered for the thermal mass, which show very different behaviour. Native regolith proved itself to be a very good thermal insulator but not the right material for the thermal mass. In the lunar rock, thanks to its better thermal conductivity, the heat is transmitted much easily from the heat source to the generator and thus, the variations in temperature of the thermal mass are larger and the temperature distribution is more homogeneous. The behaviour of the salt is between the behaviour showed by the lunar rock and the native regolith. Given its higher specific heat, the variations in temperature in the salt are lower, but the final temperature reached at the module is much lower as well. Therefore, only the lunar rock seems to be able to provide heat at a sufficiently high temperature to produce a minimum amount of electricity.

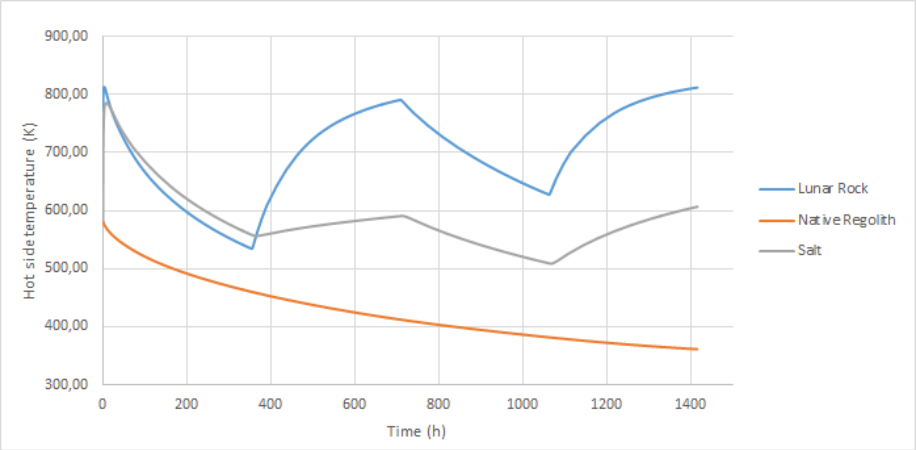

Figure 11: Temperature of the hot side of the generator during the pre-heating phase.

Fig. 12 shows the simulation results in terms of generated power and hot side temperature for the selected thermoelectric modules and the different thermal mass materials during the average length of a lunar night at the equator of the Moon.

The performance of the three considered materials is as determined by the previous analysis of the preheating. The lunar rock cools down faster than the salt, but the power generated is between 10 and 100 times larger. The thermal mass made of native regolith, as expected, shows a very poor performance.

Up to this point, despite the fact that the efficiency would affect the heat consumed to generate a given amount of power, it is not clear how it would condition the power output because, in the simulations of the modules, the amount of heat absorbed is the maximum. In the module simulations, as the heat flow was not restricted, it was not clear how the efficiency would affect the power output. Nevertheless, after the thermal mass simulations, the results (both temperature and power output) show the same behaviour. The best thermoelectric generator under the given conditions is thermocouple 2, followed by 1A and 4B. The thermoelectric generator 2 produces the largest power while absorbs less heat, hence temperature of the thermal mass decreases slower. When these results are compared to the ones in Table 1, one can observe that in principle, with unlimited heat available, the generator that produces the largest power would be 4B followed by 1A. However, this is the opposite to what happens with limited heat and actually coincides with the efficiency rating in the table. Therefore, the efficiency of the thermoelectric materials has a larger impact on their performance than expected from the previous Section. This fact is particularly important in the selection of materials for a temperature range, in which efficiency must have a major weight.

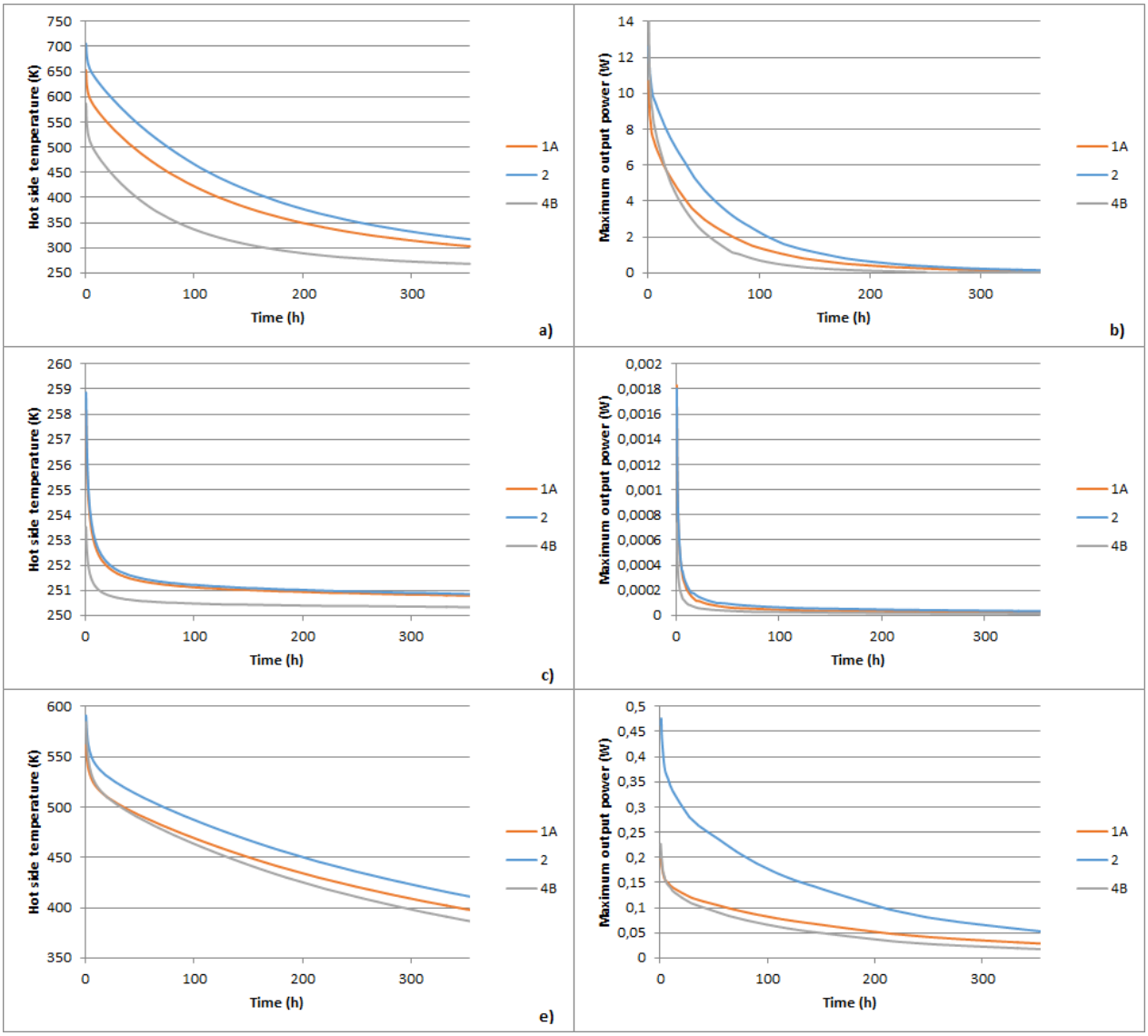

Figure 12: Time evolution of the hot side temperature of the thermoelectric generators (left) and generated power (right) for the three types of modules and thermal mass materials – Lunar rock (a, b), regolith (c, d) and salt (e, f).

The case with the largest power output (Basalt, TEG 2) produces around 12.6 W in the beginning, 4.7 W after 50 h, 2.3 W after 100 h and only 0.15 W at the end of the lunar night. The heat released by the thermal mass (volume of 0.785 m^3, mass of 227.7 kg) from 30 min after the start to 100 h later (the temperature decreases from 653 K to 422 K) is 63.13 MJ. During the same period, 1.29 MJ of electrical energy has been produced. Therefore, the overall efficiency of the system is approximately 2%. The potential ISRU generator has a similar production at the start, but the power output drops faster than the other generators, providing only 2.3 W after 50 hours, 0.7 W after 100 hours and 0.02 W in the end.

Given the power generated in the best case scenario, it seems impossible to fulfil any power demand during a whole lunar night at the equator. Even considering a case in which the system was placed in one of the advantaged points at the poles of the Moon with shorter nights (less than 100 hours [22]), the power output would still be too low. However, as the Sun incidence at these points is much lower but lasts for a longer time, no accurate comparisons can be made without a proper study of the heat source system.

Since the power output in the beginning of the night is much larger than at the end, a way to improve the system could be to stabilise the power output and thus increase the power output during the last hours. Controlling the temperature of the cold side could be a way to achieve it, as if it was not so cold in the beginning, it would reduce the amount of power generated and the heat lost as well, maintaining higher temperatures of the thermal mass for a longer time.

In [4], where similar simulations have been carried out, the generated power is 7 times larger at the beginning of the night and almost 10 times after 65 h. In these simulations, a thermal mass 2.5 times bigger and a cold sink have been modelled, which led to having a higher amount of heat stored and colder heat release temperatures. In addition, it is interesting to see that the low-temperature thermoelectric couples are in the end more suitable, for the temperature to decrease fast in the beginning and eventually remain much longer in the low-temperature levels. The study carried out in [4] is based in the same type of system and the power obtained is much higher (6 to 11 kWe), the reason being that the study is focused during the lunar day. Nevertheless, it shows that a thermal mass based system using thermoelectric generators has the capacity of generating larger amounts of power.

A final simulation has been carried out using the high temperature generators at their proper temperatures (*i.e.* heating the thermal mass up to 1200 K). The thermoelectric generator used is 1B because of its better efficiency, and the thermal mass is made of basalt, since it provided the best results in the previous simulations. Fig. 13 shows the maximum power output of this simulation and the best one reached in the previous simulations. When high temperature thermocouples are used, the power output is more than four times larger in the beginning (44 W) and more than six times larger 100 hours later (8.72 W). However, the power production at the end of the night is still very low (0.8W). Therefore, if the temperature of the thermal mass could be increased, the use of generators that can withstand it would provide a larger power. Finally, from 30 min to 100 hours, the temperature of the thermal mass decreases from 985 K to 620 K, approximately 100 MJ of heat are released producing 6.69 MJ of electricity, which means an efficiency of 6.7%, larger than before as well.

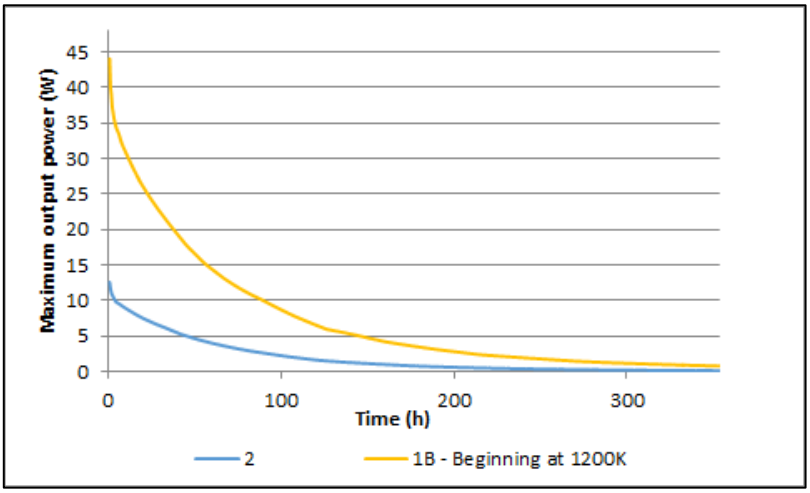

Figure 13: Maximum power output of the high temperature thermocouple simulation (yellow) and the best maximum power of the other scenarios (blue).

5. Conclusions

The application of thermoelectric modules to generate electricity in a thermal storage system in the Moon has been modelled and analysed. Several thermoelectric materials have been selected according to the temperatures that they are able to withstand in addition to some potential ISRU thermocouples. Recently studied and under research materials with good ZT have been prioritised, as to get closer to a futuristic situation with enhanced performance in terms of efficiency.

The performance of the materials has been simulated in modules and the power output and efficiency have been obtained. The results show that the maximum efficiencies are reached when the thermocouples work at the highest temperatures. With a cold side temperature of 273 K and at their maximum hot temperatures, the Nanostructured SiGe reaches an efficiency of almost 17%, BiCuSeO – SbSe/S more than 13%, and BiTeSb – BiTeSe almost 11%. However, the potential ISRU modules based on MgSi have much lower maximum efficiencies (2% to 4%).

The system with the thermal has been simulated using a selection of the thermoelectric modules, different thermal mass materials, and a constant cold side temperature. In the best case, 12.6 W of electricity have been produced in the beginning, decreasing to 4.7 W, 2.3 W and 0.15 W after 50, 100 and 364 hours, respectively. Using a thermocouple

that can endure very high temperatures, and a thermal mass at very high temperature, a power output of 44 W has been obtained in the beginning, but at the end of the lunar night the power obtained was still low (0.8 W).

Regarding the materials tested for the thermal mass, it is not possible to use the native regolith to store heat. However, basaltic rock, which can be obtained by means of regolith processing, is a good alternative.

In order to increase accuracy and have a more precise view of the possibilities of this type of system, some improvements could be done in a future work. The proper modelling of the heat source and the cold sink could significantly influence the results, as presumably the cold side temperature could be lower and thus increase the overall efficiency. In addition, taking into account the change of the properties of the thermal mass and surrounding regolith with the temperature would lead to more realistic results.

References

[1] R. Balasubramaniam, R. Wegeng, S. Gokoglu, N. Suzuki, and K. Sacksteder, "Analysis of Solar-Heated Thermal Wadis to Support Extended-Duration Lunar Exploration," *47th AIAA Aerosp. Sci. Meet.*, vol. Paper 1339, 2009.

[2] B. Climent, O. Torroba, R. González-Cinca, N. Ramachandran, and M.D. Griffin, "Heat storage and electricity generation in the Moon during the lunar night," *Acta Astronautica.*, vol. 93, pp. 352–358, 2014.

[3] M. F. Palos, P. Serra. S. Fereres, K. Stephenson, and R. González-Cinca, "Lunar ISRU energy storage and electricity generation," submitted to *Acta Astronautica*, 2019.

[4] P. Fleith *et al.*, "In-Situ Approach for Thermal Energy Storage and Thermoelectricity generation on the Moon: Modelling and Simulation,", submitted to *Planetary and Space Science*, 2019.

[5] V. Lappas, V. Kostopoulos, A. Tsourdos, and S. Kindylides, "Lunar In-situ Thermal Regolith Storage and Power Generation using Thermoelectric Generators," *AIAA SciTech Forum*, 2019.

[6] H. Lee, "Thermoelectric generators," pp. 1–12, 2006.

[7] X. W. Wang *et al.*, "Enhanced thermoelectric figure of merit in nanostructured p-type silicon germanium bulk alloys," *Nano Lett.*, vol. 8, no. 12, pp. 4670–4674, 2008.

[8] X. W. Wang *et al.*, "Enhanced thermoelectric figure of merit in nanostructured n -type silicon germanium bulk alloy," *Appl. Phys. Lett.*, vol. 93, no. 19, pp. 19–21, 2008.

[9] R. Basu *et al.*, "Improved thermoelectric performance of hot pressed nanostructured n-type SiGe bulk alloys," *J. Mater. Chem. A*, vol. 2, no. 19, p. 6922, Apr. 2014.

[10] D. Cheikh *et al.*, "Praseodymium Telluride: A High-Temperature, High-ZT Thermoelectric Material," *Joule*, vol. 2, no. 4, pp. 698–709, Apr. 2018.

[11] A. Saramat *et al.*, "Large thermoelectric figure of merit at high temperature in Czochralski-grown clathrate Ba8Ga16Ge30," *J. Appl. Phys.*, vol. 99, no. 2, p. 23708, Jan. 2006.

[12] Y.-L. Pei, H. Wu, D. Wu, F. Zheng, and J. He, "High Thermoelectric Performance Realized in a BiCuSeO System by Improving Carrier Mobility through 3D Modulation Doping," *J. Am. Chem. Soc.*, vol. 136, no. 39, pp. 13902–13908, Oct. 2014.

[13] J. Androulakis, I. Todorov, J. He, D.-Y. Chung, V. Dravid, and M. Kanatzidis, "Thermoelectrics from Abundant Chemical Elements: High-Performance Nanostructured PbSe–PbS," *J. Am. Chem. Soc.*, vol. 133, no. 28, pp. 10920–10927, Jul. 2011.

[14] K. F. Hsu *et al.*, "Cubic AgPbmSbTe2+m: Bulk Thermoelectric Materials with High Figure of Merit," *Science (80-.).*, vol. 303, no. 5659, pp. 818–821, Feb. 2004.

[15] D. Li *et al.*, "High thermoelectric performance of n-type $Bi_2Te_{2.7}Se_{0.3}$ *via* nanostructure engineering," *J. Mater. Chem. A*, 2018.

[16] H. Ihou-Mouko, C. Mercier, J. Tobola, G. Pont, and H. Scherrer, "Thermoelectric properties and electronic structure of p-type Mg2Si and Mg2Si0.6Ge0.4compounds doped with Ga," *J. Alloys Compd.*, vol. 509, no. 23, pp. 6503–6508, 2011.

[17] 2 YANG, Meijun1, Q. SHEN, X. TANG, and L. ZHANG, "Preparation of Bismuth-Doped Magnesium Silicide Material and Its Thermoelectric Properties."

[18] L. Fu *et al.*, "Thermoelectric Performance Enhancement of CeFe4Sb12 p-Type Skutterudite by Disorder on the Sb4 Rings Induced by Te Doping and Nanopores," *J. Electron. Mater.*, vol. 45, no. 3, pp. 1240–1244, Mar. 2016.

[19] J. L. Mi, X. B. Zhao, and T. J. Zhu, "Thermoelelctric properties of nanostructured skutterudite-related compounds," in *2007 26th International Conference on Thermoelectrics*, 2007, pp. 16–20.

[20] "Conductive Materials or Metal Conductivity - TIBTECH innovations -." [Online]. Available: http://www.tibtech.com/conductivity.php#metal_properties_chart. [Accessed: 09-Jun-2018].

[21] A. R. Vasavada, D. A. Paige, and S. E. Wood, "Near-Surface Temperatures on Mercury and the Moon and the Stability of Polar Ice Deposits," *Icarus*, vol. 141, no. 2, pp. 179–193, Oct. 1999.
[22] J. Fincannon, "Lunar Polar Illumination for Power Analysis," in *6th International Energy Conversion Engineering Conference (IECEC)*, 2008.